Research Square

Preprints are preliminary reports that have not undergone peer review.
They should not be considered conclusive, used to inform clinical practice,
or referenced by the media as validated information.

Outcome-blind acute metabolic displacement identifies QRS vulnerability and transient low-heart-rate susceptibility during hyperkalaemia

yiping liu
Zhengzhou University
shujie li
Jining Medical University
chao jiang
Fuwai hospital
yu hu
Fuwai hospital
ling jin
Zhengzhou University
zhe zheng
zhezheng@fuwai.com

Fuwai hospital

Research Article

Keywords: hyperkalaemia, QRS duration, heart rate, bradycardia, metabolic stress, Mahalanobis distance, MIMIC-IV, MIMIC-III

Posted Date: November 1st, 2026

DOI: https://doi.org/10.21203/rs.3.rs-10883041/v1

License: This work is licensed under a Creative Commons Attribution 4.0 International License.
Read Full License

Additional Declarations: No competing interests reported.

Abstract

Background

Electrocardiographic responses to hyperkalaemia vary substantially at similar potassium concentrations. We sought to determine whether acute displacement from a normal-potassium metabolic reference might identify the physiological context in which hyperkalaemia is associated with QRS slowing, and whether this construct could also mark acute heart-rate response or low-heart-rate burden.

Methods

We linked MIMIC-IV version 3.0 to MIMIC-IV-ECG and assembled normal-potassium–hyperkalaemia–normal-potassium ECG–laboratory trajectories. An acute metabolic displacement score (AMED) was calibrated without reference to electrophysiological outcomes in 14,400 complete normal-potassium reference trajectories, after excluding all hyperkalaemia-evaluation subjects. AMED was calculated as the shrinkage-covariance Mahalanobis distance of paired changes in creatinine, bicarbonate, and sodium, expressed per calibration standard deviation; potassium was excluded and adjusted for separately. The primary outcome in MIMIC-IV was immediate QRS change. In MIMIC-III, a separately locked post-result exploratory protocol analysed six-hour pre-event and post-event heart-rate windows. It distinguished absolute median-heart-rate response, time-weighted depth and duration below 50 beats/min, any post-event low-heart-rate exposure, and the original new sustained heart-rate-<50 endpoint. Episodes were retained, and inference was clustered by patient.

Results

The MIMIC-IV evaluation cohort comprised 1,342 complete episodes in 847 patients. Each standard deviation of AMED was associated with 0.85-ms greater immediate QRS prolongation (95% confidence interval [CI], 0.12–1.58; P = 0.022) and higher odds of dynamic QRS response (OR, 1.50; 95% CI, 1.25–1.81; false-discovery-rate P < 0.001). In MIMIC-III, 2,943 episodes from 2,409 patients had complete AMED and heart-rate windows. Each AMED standard deviation was associated with any post-event heart-rate-<50 exposure after adjustment for pre-event exposure (OR, 1.43; 95% CI, 1.14–1.80; P = 0.002; false-discovery-rate P = 0.014). The absolute median-heart-rate response was 0.42 beats/min greater per AMED standard deviation (95% CI, 0.04–0.80; nominal P = 0.029; Holm P = 0.057). AMED was not clearly associated with time-weighted low-heart-rate deficit change or the original new sustained heart-rate-<50 endpoint.

Conclusions

Outcome-blind non-potassium metabolic displacement was associated with greater QRS vulnerability and a higher probability of transient entry into a low-heart-rate state during hyperkalaemia. The pattern observed in MIMIC-III did not suggest greater cumulative or sustained bradycardic burden, which may

help distinguish threshold-entry susceptibility from persistence. These findings suggest that AMED represents a research phenotype rather than a validated bedside predictor.

Introduction

Hyperkalaemia depolarises the resting membrane potential, reduces the availability of fast sodium channels, and impairs conduction across the atria, atrioventricular node, and ventricular myocardium[1,2]. Its electrocardiographic (ECG) manifestations span a broad spectrum, ranging from subtle T or P-wave abnormalities to PR prolongation, QRS widening, bradyarrhythmias, and ultimately sine-wave degeneration. Nevertheless, a single ECG has limited sensitivity for detecting clinically significant hyperkalaemia, and patients with similar serum potassium concentrations can exhibit markedly divergent electrical phenotypes[2–5]. While QRS prolongation and bradycardia are clinically critical, signalling an elevated short-term risk, the absolute potassium concentration alone fails to predict the onset or severity of these electrophysiological derangements[4].

Prior studies have largely focused on quantifying ECG differences between normokalaemia and hyperkalaemia, correlating the magnitude of potassium elevation with specific ECG abnormalities, or employing machine learning to infer potassium levels directly from ECG tracings[6,7]. These approaches predominantly frame potassium as the primary exposure and the ECG as a passive detector. A complementary, yet underexplored, hypothesis is whether the concurrent non-potassium metabolic milieu modulates myocardial vulnerability to a potassium challenge. Conditions such as acute kidney injury, acid–base disturbances, and dysnatraemias frequently co-occur, potentially altering transmembrane gradients, modifying tissue excitability, and serving as markers of the severity and tempo of acute illness[1,2]. However, analysing these individual metabolic dimensions in isolation is inherently vulnerable to collinearity and erroneously assumes a unidirectional harmful effect for each variable. While a simple count of metabolic abnormalities offers clinical interpretability, it discards crucial information regarding the magnitude and covariance of these physiological derangements.

To address this gap, we developed the Acute Metabolic Displacement (AMED) score, an outcome-blind metric that quantifies the distance from a normal-potassium reference manifold. Crucially, the AMED score was derived exclusively from paired changes in creatinine, bicarbonate, and sodium among subjects who never entered the hyperkalaemia evaluation cohort; potassium and all electrophysiological outcomes were strictly excluded from its construction. This design allowed us to test whether a result-independent measure of departure from baseline metabolic trajectories could identify electrical vulnerability, independent of potassium severity.

A further methodological limitation in most retrospective hyperkalaemia studies is the reliance on a single, binary threshold to define bradycardia. While clinically intuitive, this approach obscures the temporal dynamics of the heart rate response—namely, whether the bradycardia is transient or sustained, the depth of the heart rate nadir, and whether the post-event rhythm fundamentally differs from the patient's pre-event baseline. These phenotypes are not clinically interchangeable. For instance,

a patient may transiently cross a threshold of 50 beats/min without accumulating a significant low-heart-rate deficit, whereas another may remain moderately bradycardic for a substantial portion of the observation window. Disentangling the magnitude of the acute response, the threshold for bradycardia, the intensity of the low-heart-rate burden, and the persistence of the state may therefore reveal distinct dimensions of underlying conduction reserve.

To evaluate this, we constructed a layered evidence chain. We first utilised the MIMIC-IV database, linked to MIMIC-IV-ECG, to assess immediate and dynamic QRS responses, establish matched normokalaemic specificity, and evaluate state–trait effects across repeated episodes[8,9]. Subsequently, we applied the MIMIC-III cohort to test the association between an interpretable multihit metabolic burden and the incidence of new-onset sustained bradycardia[10]. When direct transport of the AMED score to this rare binary endpoint proved imprecise, we pre-specified a separate, post-result exploratory protocol prior to deriving any new associations. This protocol leveraged all eligible six-hour heart-rate trajectories to disentangle the acute response magnitude from the time-weighted low-heart-rate burden and sustained bradycardia. Ultimately, we sought to determine whether the AMED score marks a general propensity for electrical instability, a specific tendency to enter a low-heart-rate state, or the persistence and depth of bradycardia once that state is established.

Methods

Study design and reporting

This retrospective observational study used deidentified data from MIMIC-IV (version 3.0), MIMIC-IV-ECG (version 1.0), and MIMIC-III (version 1.4)[8–10]. Reporting followed the STROBE and RECORD guidelines[11,12]. The original AMED components, calibration set, MIMIC-IV outcomes, covariates, multiplicity plan, and decision boundary were locked before any AMED–electrophysiology association was calculated. After the transported binary MIMIC-III endpoint proved imprecise, the acute-heart-rate protocol was explicitly designated as post-result exploratory and locked before any AMED association with the newly derived response-magnitude or time-weighted burden outcomes was calculated. Repeated eligible episodes were retained, with the patient serving as the clustering unit. No row-level controlled-access data were redistributed.

MIMIC-IV ECG-laboratory trajectories

MIMIC-IV contains deidentified hospital and intensive-care data from Beth Israel Deaconess Medical Center; MIMIC-IV-ECG provides linked diagnostic ECG waveforms, reports, and machine measurements[8,9]. Eligible ECGs were non-paced, with a QRS duration of 50–200 ms, a PR interval of 80–320 ms, and a heart rate of 30–180 beats/min. Baseline ECGs additionally required a QRS duration < 120 ms and a PR interval < 200 ms. Each ECG was paired with the nearest compatible potassium and metabolic laboratory measurements within the frozen extraction windows. A hyperkalaemia trajectory

comprised: (1) a baseline ECG paired with a potassium level of 3.5-5.0 mmol/L; (2) a subsequent challenge ECG paired with a potassium level ≥ 5.5 mmol/L; and (3) a recovery ECG paired with a potassium level of 3.5-5.0 mmol/L. The baseline ECG was obtained within 30 days before the challenge, and the recovery ECG within 7 days after. All qualifying trajectories were retained, with episodes clustered by patient. Immediate QRS change was defined as the stress QRS minus the baseline QRS. Maximum QRS prolongation was the maximum of zero, the immediate change, and the recovery QRS minus the baseline QRS. A dynamic QRS response was defined as a maximum prolongation ≥ 10 ms. This threshold represents a research phenotype and not a treatment cutoff.

Outcome-blind AMED calibration

The calibration cohort consisted of independent normal-potassium ECG-laboratory trajectories. Every subject appearing in the hyperkalaemia evaluation set was excluded before calibration. The core vector contained: (1) log(creatinine at stress / creatinine at baseline); (2) bicarbonate at stress minus bicarbonate at baseline; and (3) sodium at stress minus sodium at baseline. For each component, values were winsorised at the 0.5th and 99.5th percentiles of the calibration data and centred at the calibration median. A Ledoit-Wolf shrinkage covariance matrix was estimated from the centred vectors[13]. Raw AMED was the square root of the corresponding Mahalanobis quadratic form and was divided by its standard deviation in the calibration cohort. Thus, the reported effect represents one calibration-standard-deviation greater displacement. The distance is non-directional: it measures the joint magnitude of departure without estimating outcome-optimised weights. Potassium was never a component of AMED and remained a separate model covariate. The calibration cohort contained 14,716 trajectories before complete-case selection and 14,400 with the core vector. The locked medians, winsorisation limits, covariance matrix, and scale were applied unchanged to the MIMIC-IV evaluation, matched normal-potassium, and MIMIC-III data. An expanded sensitivity score added the log urea-nitrogen ratio and changes in total calcium and magnesium but required complete data for all six components.

Primary and secondary MIMIC-IV models

The primary model regressed immediate QRS change on core AMED using a linear independence-working generalized estimating equation with a patient-clustered sandwich covariance[14]. It adjusted for age per 10 years, sex, challenge potassium severity per 0.5 mmol/L above 5.0, baseline QRS per 10 ms, log(1 + days from baseline to challenge), and stress heart rate per 10 beats/min. The key secondary logistic model used the same exposure and covariates for dynamic QRS response. Secondary continuous outcomes were signed potassium-QRS loop area, immediate PR change, and immediate heart-rate slowing. Benjamini-Hochberg correction was applied to the prespecified secondary AMED family; the immediate-QRS model was the single primary test. Observed dynamic-response risks were summarised across AMED quartiles with Wilson 95% confidence intervals. Robustness analyses excluded the highest 1% of AMED values, excluded the outer 1% of immediate QRS changes, restricted

the ECG-potassium lag to ≤ 3 hours, and recalibrated AMED after additionally excluding every subject represented in the matched normal-potassium control set. A post-result reviewer-challenge analysis entered continuous AMED and the simple 0–3 burden simultaneously; it was labelled a sensitivity analysis rather than a new primary model.

Matched normal-potassium specificity

The frozen matching pipeline paired each primary hyperkalaemia trajectory with one normal–normal–normal potassium trajectory without using subsequent QRS outcomes. Matching was without replacement, exact on sex, and based on age, baseline QRS, PR, heart rate, baseline estimated glomerular filtration rate (eGFR), trajectory intervals, and propensity-score logit; balance was assessed using standardised differences[15]. The locked AMED transformation was applied to both groups. A match-clustered linear model included the exposure group, AMED, and their interaction, together with the primary covariates. The interaction estimated the difference in the AMED-QRS slope between hyperkalaemia and normal-potassium states. eGFR was calculated using the 2021 race-free creatinine Eq. 1[6]. As a separate exposure-specificity analysis, dynamic QRS response risk during hyperkalaemia was compared with matched serial normal-potassium variation. Paired risk differences used 2,000 pair-level bootstrap samples, and discordant pairs were tested with exact McNemar tests.

Interpretable multihit and state–trait analyses

The core acute stress burden counted three abnormalities: an acute-kidney-injury-compatible creatinine change (increase ≥ 0.3 mg/dL within 48 hours or ≥ 1.5-fold within 7 days), bicarbonate < 22 mmol/L, and sodium < 135 or > 145 mmol/L. The expanded count additionally included total calcium < 8.5 mg/dL and magnesium < 1.7 mg/dL. Logistic models for dynamic QRS response adjusted for age, sex, baseline QRS, PR, and heart rate, potassium severity, challenge eGFR, and trajectory intervals. To separate acute episode variation from stable between-patient differences, the 0–3 burden was decomposed using a Mundlak model into the patient-mean burden (trait) and each episode's deviation from that mean (state)[17]. Both terms were entered together with the locked covariates. A patient fixed-effects analysis among patients with repeated episodes served as a within-person sensitivity analysis.

MIMIC-III clinical-consequence analysis

MIMIC-III provided a legacy temporal and modality-level test using charted heart rate rather than diagnostic ECG intervals[10]. Hyperkalaemia was anchored at a potassium level ≥ 5.5 mEq/L. Heart rates of 20–250 beats/min were retained, duplicate measurements at the same chart time were collapsed to their median, and each episode required at least three distinct chart times in both the six hours before and the six hours after the potassium measurement. The locked MIMIC-IV AMED transformation was applied without recalibration. The exploratory heart-rate redesign separated four phenotype dimensions. Acute response magnitude was the absolute difference between post-event and pre-event median heart

rate. The time-weighted low-heart-rate deficit integrated max(50 − 0) over each six-hour window using linear interpolation; the nearest in-window observation was carried to each window boundary. Dividing the integral by six hours yielded the mean depth below 50 beats/min. The low-heart-rate time fraction was the interpolated proportion of the window below 50 beats/min, and any low-heart-rate burden indicated a non-zero post-event fraction. The original new sustained bradycardia definition-at least two distinct post-event readings < 50 beats/min, no sustained pre-event bradycardia, and at least three readings in each window-was retained unchanged. Two co-primary exploratory outcomes were fixed: absolute median-heart-rate response and post-minus-pre time-weighted low-heart-rate deficit. Continuous outcomes used linear models with patient-clustered sandwich covariance. Fractional low-heart-rate time used fractional logit, and any low-heart-rate burden and new sustained bradycardia used logistic regression with patient-clustered covariance. Models adjusted for age per 10 years, sex, potassium severity per 0.5 mEq/L, pre-event median heart rate per 10 beats/min, and log-transformed numbers of pre-event and post-event chart times. Post-event low-heart-rate models additionally adjusted for the corresponding pre-event burden. The two co-primary P values were Holm adjusted. Six secondary heart-rate phenotypes formed a Benjamini-Hochberg family. Sensitivity analyses retained the first complete heart-rate episode per patient and decomposed AMED into patient-mean and episode-specific components using a Mundlak model. The original missing-data analyses were also retained: 40 outcome-free chained-equation imputations, first-episode Firth penalised logistic regression with profile penalised-likelihood inference[18], and a calibration-scaled directional metabolic index. None replaced the original transported estimate or the newly locked exploratory family.

Statistical analysis and reproducibility

Two-sided 95% CIs and P values are reported, with effect size and precision prioritised over significance labels. Repeated observations used patient-clustered sandwich covariance; matched analyses clustered by match. The original MIMIC-IV secondary family used Benjamini-Hochberg correction; the new MIMIC-III co-primary family used Holm correction, and its secondary family used Benjamini–Hochberg correction. Complete cases were used for each locked score because AMED requires all component changes. Individual heart-rate readings were used only to construct episode-level summaries and were never treated as independent observations. Deterministic preprocessing, calibration parameters, analytic cohorts, model tables, source data, and cryptographic hashes were saved. Independent reruns reproduced all seven original AMED audit hashes and all four new acute-heart-rate result hashes;prespecified original integrity checks passed[19].

Results

Cohort and outcome-blind score construction

The normal-potassium reference cohort contained 14,716 trajectories from 14,716 subjects, after excluding all subjects from the hyperkalaemia evaluation set. Of these, 14,400 (97.9%) had complete

data for the core AMED components. The MIMIC-IV evaluation set comprised 1,356 hyperkalaemia trajectories from 858 patients; 1,342 episodes in 847 patients had complete core AMED data (Fig. 1; Table 1). The median age was 61 years, 48.3% of episodes were in women, the median challenge potassium was 5.9 mmol/L, and 257 episodes (19.2%) met the threshold for dynamic QRS response.

Table 1
MIMIC-IV evaluation cohort and extreme AMED quartiles

Characteristic	**Overall (1,342 episodes; 847 patients)**	**AMED Q1 (336 episodes)**	**AMED Q4 (336 episodes)**
Age, years	61 [5–71]	62 [52–71]	58 [48–69]
Female	648 (48.3%)	151 (44.9%)	162 (48.2%)
Baseline potassium, mmol/L	4.4 [4.0-4.7]	4.5 [4.1–4.8]	4.3 [3.9–4.7]
Challenge potassium, mmol/L	5.9 [5.6–6.3]	5.9 [5.6–6.3]	5.9 [5.6–6.2]
Baseline QRS, ms	90 [82–98]	90 [82–98]	90 [82–96]
Immediate QRS change, ms	0 [-4 to 4]	0 [-4 to 4]	2 [-4 to 8]
Maximum QRS prolongation, ms	2 [0–8]	2 [0–6]	4 [0–10]
Baseline creatinine, mg/dL	1.40 [0.90–2.88]	1.20 [0.80–2.23]	1.45 [0.90–3.70]
Challenge creatinine, mg/dL	1.70 [1.00-3.70]	1.40 [0.90–2.40]	2.60 [1.48–4.72]
Baseline bicarbonate, mmol/L	25 [22–28]	24 [22–27]	26 [22–28]
Challenge bicarbonate, mmol/L	22 [19–26]	24 [21–26]	20 [17–25]
Baseline sodium, mmol/L	138 [135–141]	138 [135–141]	138 [135–141]
Challenge sodium, mmol/L	136 [132–139]	137 [134–139]	133 [128–138]
Core 0–3 stress burden	1 [0–2]	1 [0–1]	2 [1–2]
AMED, calibration SD units	2.09 [1.39–2.95]	1.01 [0.71–1.24]	3.42 [3.17–3.75]
Dynamic QRS response ≥ 10 ms	257 (19.2%)	46 (13.7%)	97 (28.9%)

Values are median [interquartile range] or n (%). Rows are episodes; patients may contribute more than one episode. AMED, acute metabolic displacement; Q, quartile.

AMED captured coordinated metabolic shifts not reflected by the potassium level alone. Across the extreme AMED quartiles, the median challenge potassium was identical at 5.9 mmol/L, while the median stress creatinine increased from 1.40 to 2.60 mg/dL, stress bicarbonate decreased from 24 to 20 mmol/L, and stress sodium decreased from 137 to 133 mmol/L (Table 1). AMED showed a moderate correlation with the 0–3 abnormality count (Pearson r = 0.37), indicating conceptual overlap but not equivalence.

AMED and QRS vulnerability during hyperkalaemia

In the prespecified primary model, each standard deviation (SD) increase in AMED was associated with 0.85 ms greater immediate QRS prolongation (95% CI, 0.12–1.58; P = 0.022; Fig. 2b; Table 2). This association was robust across multiple sensitivity analyses: after excluding the highest 1% of AMED values (+ 0.98 ms; 95% CI, 0.24–1.73), excluding the outer 1% of immediate QRS changes (+ 0.76 ms; 95% CI, 0.15–1.37), restricting the ECG-potassium time lag to ≤ 3 hours (+ 1.11 ms; 95% CI, 0.19–2.02), and applying a stricter outcome-independent calibration (+ 0.86 ms; 95% CI, 0.15–1.57).

Table 2
Positive evidence chain

Evidence layer	Analysis	n/events	Effect (95% CI)	P value
Outcome-blind primary association	AMED → immediate QRS change	1,342 episodes	+ 0.85 ms/SD (0.12–1.58)	0.022
Threshold phenotype	AMED → dynamic QRS response ≥ 10 ms	1,342/257	OR 1.50/SD (1.25–1.81)	< 0.001; FDR < 0.001
Dose gradient	Q4 versus Q1 observed response risk	97/336 vs 46/336	28.9% vs 13.7%	Descriptive
Matched state specificity	Hyperkalaemia-by-AMED interaction	2,307 trajectories	+ 0.87 ms/SD (0.15–1.59)	0.018; FDR 0.107
Calibration robustness	Strict-calibration interaction	2,307 trajectories	+ 0.85 ms/SD (0.15–1.56)	0.018
Increment beyond hit count	AMED mutually adjusted for core burden	1,342/257	OR 1.31/SD (1.07–1.61)	0.009
Interpretable construct	Core burden → dynamic QRS response	841/154	OR 1.45/hit (1.16–1.80)	0.001
Within-patient state	Episode burden deviation → maximum QRS prolongation	1,349 episodes; 852 patients	+ 1.66 ms/hit (0.37–2.96)	0.012; FDR 0.047
Clinical consequence	MIMIC-III core burden → new sustained HR < 50	2,943/30	OR 1.51/hit (1.07–2.15)	0.020
Clinical-consequence sensitivity	MIMIC-III first eligible episode	2,187/24	OR 1.77/hit (1.22–2.57)	0.003
Transient rate susceptibility	Locked AMED → any post-event HR < 50 burden	2,943/99	OR 1.43/SD (1.14–1.80)	0.002; FDR 0.014
Descriptive threshold gradient	AMED Q4 versus Q1 observed post-event HR < 50 risk	38/736 vs 17/737	5.2% vs 2.3%	Descriptive; middle quartiles non-monotonic

CI, confidence interval; FDR, false-discovery-rate-adjusted P value; HR, heart rate; OR, odds ratio; SD, calibration standard deviation.

The association was more pronounced in the threshold analysis. Each SD of AMED was associated with 50% higher odds of a dynamic QRS response (OR, 1.50; 95% CI, 1.25–1.81; P < 0.001; false-discovery-rate P < 0.001). The observed risk of response increased from 46 of 336 episodes (13.7%) in the lowest

AMED quartile to 97 of 336 (28.9%) in the highest quartile (Fig. 2a). In a reviewer-challenge model that included both continuous AMED and the simple 0–3 burden count, AMED remained associated with dynamic response (OR, 1.31; 95% CI, 1.07–1.61), as was each additional core burden hit (OR, 1.41; 95% CI, 1.14–1.76; Fig. 2c). However, in a mutually adjusted model for the continuous immediate-QRS outcome, the simple hit count, not AMED, was the significant predictor, suggesting the two metrics capture related but distinct aspects of the response.

Hyperkalaemia-state specificity

In the matched interaction model, which included 2,307 scored trajectories, the AMED-QRS slope was −0.27 ms per SD during normal potassium states (95% CI, -0.69 to 0.15) and + 0.60 ms during hyperkalaemia (95% CI, -0.002 to 1.20). The interaction term was + 0.87 ms (95% CI, 0.15–1.59; nominal P = 0.018; Fig. 2d), indicating a steeper slope during hyperkalaemia. The interaction using the strict-calibration AMED was nearly identical (+ 0.85 ms; 95% CI, 0.15–1.56). Although the prespecified family-wise false-discovery-rate P value for this interaction was 0.107, its direction and magnitude are consistent with an enrichment of the AMED association specifically during the potassium challenge.

Exposure specificity was also evident using the threshold phenotype. A dynamic QRS response occurred in 18.2% of primary hyperkalaemia trajectories versus 14.3% of their matched normal-potassium trajectories, a paired risk difference of 3.9 percentage points (95% CI, 0.4–7.6; P = 0.036). For an empirical normal-potassium tail threshold of > 16 ms, the paired risk difference was 2.5 percentage points (95% CI, 0.2–4.6; P = 0.044; Fig. 3a).

Interpretable burden and within-patient state evidence

The findings for the outcome blind distance metric were supported by a clinically transparent stress count. Among complete cases from the primary episode, each additional kidney bicarbonate sodium hit was associated with higher odds of dynamic QRS response (OR, 1.45; 95% CI, 1.16–1.80; P = 0.001). The expanded five-component burden yielded a similar result (OR, 1.35; 95% CI, 1.11–1.65; P = 0.003; Fig. 3b). Each core hit was also associated with 1.01-ms greater maximum QRS prolongation (95% CI, 0.21–1.80; P = 0.013).

When analyzing all eligible repeated trajectories, a one-hit deviation above a patient's own mean burden was associated with 1.66 ms greater maximum QRS prolongation (95% CI, 0.37–2.96; false-discovery-rate P = 0.047). A patient fixed-effects analysis yielded an identical estimate (+ 1.66 ms; 95% CI, 0.37–2.96). The between-patient (trait) estimate was smaller (+ 0.85 ms; 95% CI, 0.02–1.68; false-discovery-rate P = 0.088), although the difference between the state and trait effects was not statistically significant (Fig. 3c). These models support an acute, within-patient component to the risk without proving it exceeds all stable, between-patient susceptibility.

Acute heart-rate response and low-heart-rate burden in MIMIC-III

The original analysis using the interpretable core burden included 2,943 complete episodes in 2,406 patients, with 30 events of new sustained bradycardia (heart rate < 50). Each additional kidney–bicarbonate–sodium hit was associated with new sustained bradycardia (OR, 1.51; 95% CI, 1.07–2.15; P = 0.020; Fig. 3d), with consistent results across first-episode, available-component, and weighting analyses. This supports the broader multihit construct but does not directly validate the continuous AMED transformation.

The new AMED heart-rate cohort contained 2,943 episodes from 2,409 patients; 371 patients contributed more than one eligible episode. Ninety-nine episodes had any post-event time with a heart rate below 50 beats/min, compared with 66 in the pre-event window. The observed post-event risk was 2.3% (17/737) in AMED quartile 1 and 5.2% (38/736) in quartile 4, with no monotonic trend across the middle quartiles (Fig. 4b). After adjusting for pre-event low-heart-rate exposure and other covariates, each SD of AMED was associated with higher odds of any post-event heart-rate-<50 burden (OR, 1.43; 95% CI, 1.14–1.80; P = 0.002; false-discovery-rate P = 0.014; Fig. 4d). The fractional time spent below 50 beats/min was directionally consistent (fractional OR, 1.48; 95% CI, 1.03–2.11; nominal P = 0.034) but did not remain significant after correction for the secondary family (false-discovery-rate P = 0.101).

Each SD of AMED corresponded to a 0.42-beats/min larger absolute median-heart-rate response (95% CI, 0.04–0.80; nominal P = 0.029), although the Holm-adjusted co-primary P value was 0.057 (Fig. 4c). The first-episode estimate was similar (+ 0.46 beats/min; 95% CI, 0.02–0.90). In the state–trait model, the between-patient AMED component was associated with response magnitude (+ 0.45 beats/min; 95% CI, 0.03–0.87), whereas the within-patient component was imprecise (+ 0.27 beats/min; 95% CI, -0.46 to 1.00). AMED was not clearly associated with the change in time-weighted low-heart-rate deficit (+ 0.03 beats/min; 95% CI, -0.02 to 0.08; Holm P = 0.210) or the original new sustained heart-rate-<50 endpoint (OR, 1.27; 95% CI, 0.83–1.96). Thus, the multiplicity-robust signal in MIMIC-III concerned the entry into a low-heart-rate state, rather than the accumulated depth or sustained persistence of that state.

Boundary and exploratory sensitivity analyses

Several analyses did not provide confirmatory evidence and are reported together to define the boundaries of the study's claims (Table 3; Figure S1; Supplementary Tables S3–S4). Core AMED was not associated with the signed potassium–QRS loop area, immediate PR change, immediate heart-rate slowing, or the expanded complete-case QRS score. The AMED state–trait decomposition did not resolve a within-patient effect on immediate QRS change. In MIMIC-III, outcome-free multiple imputation did not strengthen the original sustained-bradycardia estimate, and the first-episode Firth estimate was nominally positive but not robust to multiplicity correction. The new response-magnitude co-primary result was also nominal rather than Holm-significant, while burden intensity and sustained bradycardia remained uncertain. These findings preclude interpreting AMED as a validated cross-database predictor or as a measure of bradycardia duration.

Table 3
Boundary and exploratory sensitivity analyses

Analysis	n/events	Effect (95% CI)	P value/interpretation
AMED → signed potassium–QRS loop area	1,342	+ 0.43 units/SD (− 0.23 to 1.08)	0.205; FDR 0.532
AMED → immediate PR change	1,342	+ 0.31 ms/SD (− 1.26 to 1.87)	0.701; FDR 0.760
AMED → immediate heart-rate slowing	1,342	+ 0.79 beats/min/SD (− 0.26 to 1.84)	0.141; FDR 0.458
Expanded AMED → immediate QRS change	780	+ 0.56 ms/SD (-0.52 to 1.65)	0.308; FDR 0.540
Within-patient AMED state → immediate QRS change	1,342	+ 0.48 ms/SD (-1.11 to 2.06)	0.554; FDR 0.721
Locked AMED → MIMIC-III new sustained HR < 50	2,912/31	OR 1.27/SD (0.83–1.96)	0.271
Locked AMED → MIMIC-III minimum HR change	2,943	−0.05 beats/min/SD -0.60 to 0.49)	0.847
Locked AMED → absolute median-HR response	2,943	+ 0.42 beats/min/SD (0.04–0.80)	0.029; Holm 0.057
Locked AMED → time-weighted HR < 50 deficit change	2,943	+ 0.03 beats/min/SD (-0.02 to 0.08)	0.210; Holm 0.210
Locked AMED → post-event time fraction HR < 50	2,943	Fractional OR 1.48/SD (1.03–2.11)	0.034; FDR 0.101
Locked AMED → MIMIC-III HR < 50, first episode	2,141/26	OR 1.50/SD (0.94–2.39)	0.091
Outcome-free MI AMED → MIMIC-III HR < 50	7,897/56	OR 1.19/SD (0.82–1.72)	0.354; FDR 0.354
Firth AMED → MIMIC-III HR < 50, first episode	2,141/26	OR 1.50/SD (1.01–2.21)	0.046; FDR 0.137
Directional AMDI → MIMIC-III HR < 50	2,912/31	OR 1.24/SD (0.95–1.62)	0.113; FDR 0.169

Boundary analyses are reported to prevent selective outcome reporting; they are not used to support the main claim.

Discussion

This study identifies acute, non-potassium metabolic displacement as a measurable correlate of electrical vulnerability during hyperkalaemia. The central evidence chain is built on four key observations. First, an outcome-blind score derived exclusively from normal-potassium metabolic trajectories was

associated with continuous immediate QRS prolongation in the MIMIC-IV cohort. Second, this association was more pronounced for a clinically interpretable dynamic threshold (≥ 10 ms QRS prolongation), with the observed risk more than doubling between the lowest and highest AMED quartiles, despite similar median potassium levels. Third, matched normal-potassium trajectories and within-patient analyses localized the QRS signal to the acute hyperkalaemic challenge, rather than to ordinary serial ECG variation. Fourth, in the MIMIC-III cohort, the locked AMED score was associated with the probability of transiently entering a low-heart-rate state (< 50 beats/min) but was not clearly associated with the cumulative depth or sustained persistence of bradycardia. This defines a narrower phenotype of transient threshold-entry susceptibility, distinct from sustained conduction system depression.

The primary innovation is the use of an outcome-blind metric. By calibrating AMED without any QRS or heart-rate data and explicitly excluding potassium, the design reduces the risk that the score merely rediscovers the analyzed electrical endpoint. The findings suggest that the metabolic context in which a potassium challenge occurs is a critical determinant of the myocardial response.

Hyperkalaemia slows myocardial conduction by depolarizing the resting membrane potential and reducing the availability of fast sodium channels. However, the clinical ECG phenotype is highly heterogeneous at any given potassium concentration[21]. Acute kidney dysfunction, acid-base disturbances, and dysnatraemia are common co-occurring stressors that can alter the physiological environment and myocardial excitability. AMED operationalizes this environment as a multivariate displacement, capturing the joint magnitude and covariance of metabolic change.

The moderate correlation between AMED and a simple abnormality count, and the fact that both remained associated with dynamic QRS response in mutually adjusted models, suggests they capture related but non-identical information. The count offers clinical interpretability, while AMED retains graded, covariance-aware information about the metabolic trajectory. Their agreement strengthens the evidence for the underlying construct.

The absolute effect sizes, while statistically significant, are modest (e.g., ~ 0.85 ms QRS prolongation per AMED SD). The more informative observation is the distributional shift: the adjusted odds of a ≥ 10ms dynamic QRS response rose by 50% per SD increase in AMED. The pattern in MIMIC-III was analogous but more sharply bounded. The probability of any post-event low-heart-rate burden was robust to multiplicity correction, whereas the association with the magnitude of heart-rate change was nominal (Holm-adjusted P = 0.057). This combination is compatible with a model where a displaced metabolic state increases the probability of brief, transient excursions below a physiological threshold in a susceptible subset, rather than causing a uniform slowing across the entire cohort[17].

The matched analysis provides a critical specificity test. If AMED merely marked noisy laboratory sampling or general ECG variability, a similar association would be expected during normal-potassium trajectories. Instead, the interaction estimate favored a stronger AMED-QRS relationship specifically

during hyperkalaemia. Although this interaction did not retain statistical significance after correction for the full secondary family, its direction and magnitude are coherent with the primary QRS association and the observed quartile gradient.

Repeated episodes offer a different form of control. A patient's deviation above their own typical multihit burden was associated with greater maximum QRS prolongation, and a patient fixed-effects model reproduced this estimate. This reduces-but cannot eliminate confounding by stable patient characteristics. The data support an acute "state" component to the risk but do not prove it exceeds all stable, between patient "trait" susceptibility. A useful conceptual model is therefore state dependent expression on a heterogeneous substrate.

The MIMIC-III analysis adds a complementary layer of support and distinction. The simple multihit count predicted new sustained bradycardia, whereas the continuous AMED score identified any post-event low-heart-rate exposure. This suggests the threshold count may be better aligned with persistent conduction depression, while the Mahalanobis distance marks a broader, more labile substrate prone to transient instability. The state–trait analysis further refines this interpretation: the absolute heart-rate response was more clearly related to the between-patient (trait) AMED component, unlike the within-patient (state) result for QRS prolongation. This indicates that stable factors like chronic kidney disease or structural heart disease may contribute to the heart-rate association, and the result should not be interpreted as proof that an acute rise in AMED causes a fall in heart rate.

These findings argue against interpreting potassium concentration as a complete electrophysiological dose. The surrounding metabolic trajectory provides additional context that may help explain why similar potassium values produce different ECG responses. Clinically, this supports integrated serial assessment over reliance on a single potassium result or a single ECG. However, the results do not suggest that AMED should be used to trigger monitoring or treatment; urgent hyperkalaemia management should continue to follow established guidelines based on clinical presentation, potassium severity, and ECG findings[18,20,22].

For research, AMED provides a reproducible, outcome-blind method to define the acute metabolic context of a potassium challenge. Future prospective studies should collect continuous telemetry alongside synchronized ECG, laboratory, and treatment data. The central external test is now explicit: to determine whether a locked AMED score can predict threshold entry, time below threshold, depth below threshold, and sustained conduction events as separable outcomes in an independent cohort. Only after such validation should AMED be considered for use in clinical prediction.

Strengths and Limitations

Strengths of this study include the complete separation of score calibration from outcome evaluation, the exclusion of potassium from the AMED score, the use of matched normal-potassium controls, and the explicit separation of different dimensions of heart rate response (magnitude, threshold entry,

burden, persistence). The design directly addresses a gap left by studies that only compare potassium categories or compress a time series into a single binary endpoint.

Several limitations define the boundary of inference. First, the retrospective, observational design is subject to residual confounding by illness severity, medications, and other unmeasured factors. Second, the data are from a single institution, and the different eras of MIMIC-III and MIMIC-IV do not constitute geographic external validation. Third, the acute-heart-rate redesign in MIMIC-III was a post-result exploratory analysis; its co-primary response-magnitude estimate was nominally positive but did not meet the Holm-adjusted significance threshold. This finding requires independent confirmation. Fourth, low-heart-rate burden was reconstructed from intermittently charted vital signs, which cannot replicate the fidelity of continuous telemetry. Finally, the average QRS and heart rate effects were small, and retrospective association cannot establish causality or define clinical treatment thresholds.

Declarations

Ethics statement

This secondary analysis used deidentified or publicly distributed datasets under their respective access and data-use conditions. Dataset-specific ethics and consent statements are reported by the original studies. The authors should insert the institutional determination for the combined secondary analysis before submission.

Clinical trial number

Not applicable

Competing interests

The authors declare no competing interests.

Funding

No funding.

Author Contribution

Yiping Liu participated in the analysis tools, data collection and analysis, and wrote the paper. Shujie Li was responsible for the research design. Jiang Chao, Yu Hu, and Lin Jin were responsible for chart revision. Zhe Zheng was responsible for modifying the paper.

Acknowledgements

The authors thank the participants and investigators of NHANES III, MIMIC-IV.

Data Availability

The datasets analyzed during the current study are publicly available. The NHANES III data are available from the National Center for Health Statistics (NCHS). The MIMIC-IV database is available from PhysioNet. The CHARLS data are available from the China Health and Retirement Longitudinal Study official website. The atrial transcriptomic datasets analyzed during the current study are available in the Gene Expression Omnibus (GEO) repository.

References

1. Palmer BF, Carrero JJ, Clegg DJ et al. Clinical management of hyperkalemia. Mayo Clin Proc. 2021;96(3):744–762. 10.1016/j.mayocp.2020.06.014
2. Palmer BF, Clegg DJ. Electrophysiological and clinical consequences of hyperkalemia. Kidney Int Suppl. 2016;6(1):16–9. 10.1016/j.kisu.2016.01.003.
3. Montford JR, Linas S. How dangerous is hyperkalemia? J Am Soc Nephrol. 2017;28(11):3155–65. 10.1681/ASN.2016121344.
4. Durfey N, Lehnhof B, Bergeson A, et al. Severe hyperkalemia: can the electrocardiogram risk stratify for short-term adverse events? West J Emerg Med. 2017;18(5):963–71. 10.5811/westjem.2017.6.33033.
5. Montague BT, Ouellette JR, Buller GK. Retrospective review of the frequency of ECG changes in hyperkalemia. Clin J Am Soc Nephrol. 2008;3(2):324–30. 10.2215/CJN.04611007.
6. Tsai C, Patel H, Horbal P, et al. Comparison of quantifiable electrocardiographic changes associated with severe hyperkalemia. Int J Cardiol. 2023;391:131257. 10.1016/j.ijcard.2023.131257.
7. Nakayama T, Mitsuno R, Azegami T, et al. Baseline potassium levels and their association with electrocardiograph abnormalities in hyperkalaemia. Nephrol (Carlton). 2025;30(3):e70100. 10.1111/nep.70100.
8. Johnson AEW, Bulgarelli L, Shen L, et al. MIMIC-IV, a freely accessible electronic health record dataset. Sci Data. 2023;10(1):1. 10.1038/s41597-022-01899-x.
9. Gow B, Pollard T, Nathanson LA et al. MIMIC-IV-ECG: diagnostic electrocardiogram matched subset. Version 1.0. PhysioNet. 2023. 10.13026/4nqg-sb35
10. Johnson AEW, Pollard TJ, Shen L, et al. MIMIC-III, a freely accessible critical care database. Sci Data. 2016;3:160035. 10.1038/sdata.2016.35.
11. von Elm E, Altman DG, Egger M, et al. The Strengthening the Reporting of Observational Studies in Epidemiology (STROBE) statement. Ann Intern Med. 2007;147(8):573–7. 10.7326/0003-4819-147-8-

200710160-00010.
12. Benchimol EI, Smeeth L, Guttmann A, et al. The REporting of studies Conducted using Observational Routinely-collected health Data (RECORD) statement. PLoS Med. 2015;12(10):e1001885. 10.1371/journal.pmed.1001885.
13. Ledoit O, Wolf M. A well-conditioned estimator for large-dimensional covariance matrices. J Multivar Anal. 2004;88(2):365–411. 10.1016/S0047-259X(03)00096-4.
14. Liang KY, Zeger SL. Longitudinal data analysis using generalized linear models. Biometrika. 1986;73(1):13–22. 10.1093/biomet/73.1.13.
15. Austin PC. Balance diagnostics for comparing the distribution of baseline covariates between treatment groups in propensity-score matched samples. Stat Med. 2009;28(25):3083–107. 10.1002/sim.3697.
16. Inker LA, Eneanya ND, Coresh J, et al. New creatinine- and cystatin C-based equations to estimate GFR without race. N Engl J Med. 2021;385(19):1737–49. 10.1056/NEJMoa2102953.
17. Mundlak Y. On the pooling of time series and cross section data. Econometrica. 1978;46(1):69–85. 10.2307/1913646.
18. Heinze G, Schemper M. A solution to the problem of separation in logistic regression. Stat Med. 2002;21(16):2409–19. 10.1002/sim.1196.
19. Bakris G, Agiro A, Mu F, et al. Consequences of recurrent hyperkalemia on cardiovascular outcomes and mortality. JACC Adv. 2024;3(11):101331. 10.1016/j.jacadv.2024.101331.
20. Drumheller BC, Tuffy E, Gibney F, et al. Severe bradycardia from severe hyperkalemia: patient characteristics, outcomes and factors associated with hemodynamic support. Am J Emerg Med. 2022;55:117–25. 10.1016/j.ajem.2022.03.007.
21. Raffee LA, Alawneh KZ, Ababneh MJ, et al. Clinical and electrocardiogram presentations of patients with high serum potassium concentrations within emergency settings: a prospective study. Int J Emerg Med. 2022;15(1):23. 10.1186/s12245-022-00422-8.
22. Rafique Z, Peacock WF, Armstead T, et al. Hyperkalemia management in the emergency department: an expert panel consensus. J Am Coll Emerg Physicians Open. 2021;2(6):e12572. 10.1002/emp2.12572.

Figures

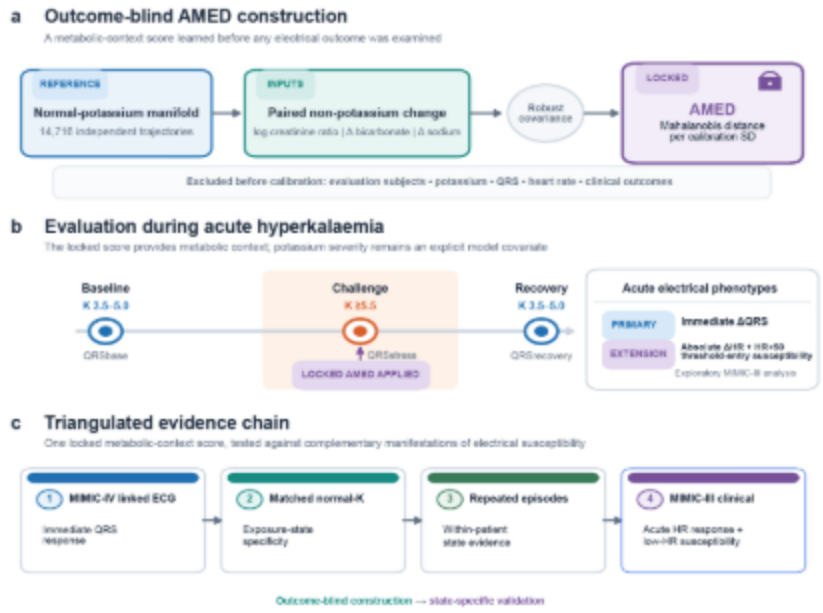


Figure 1

Outcome-blind AMED construction and the prespecified evidence chain. Potassium and all electrophysiological outcomes were excluded from score calibration.

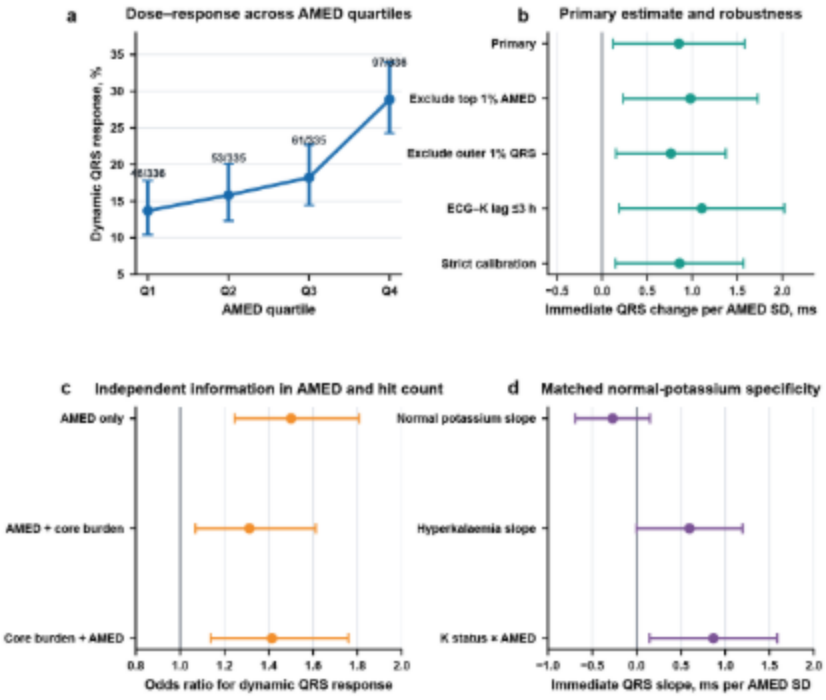


Figure 2

AMED identifies QRS vulnerability during hyperkalaemia. Points show estimates and lines show 95% confidence intervals.

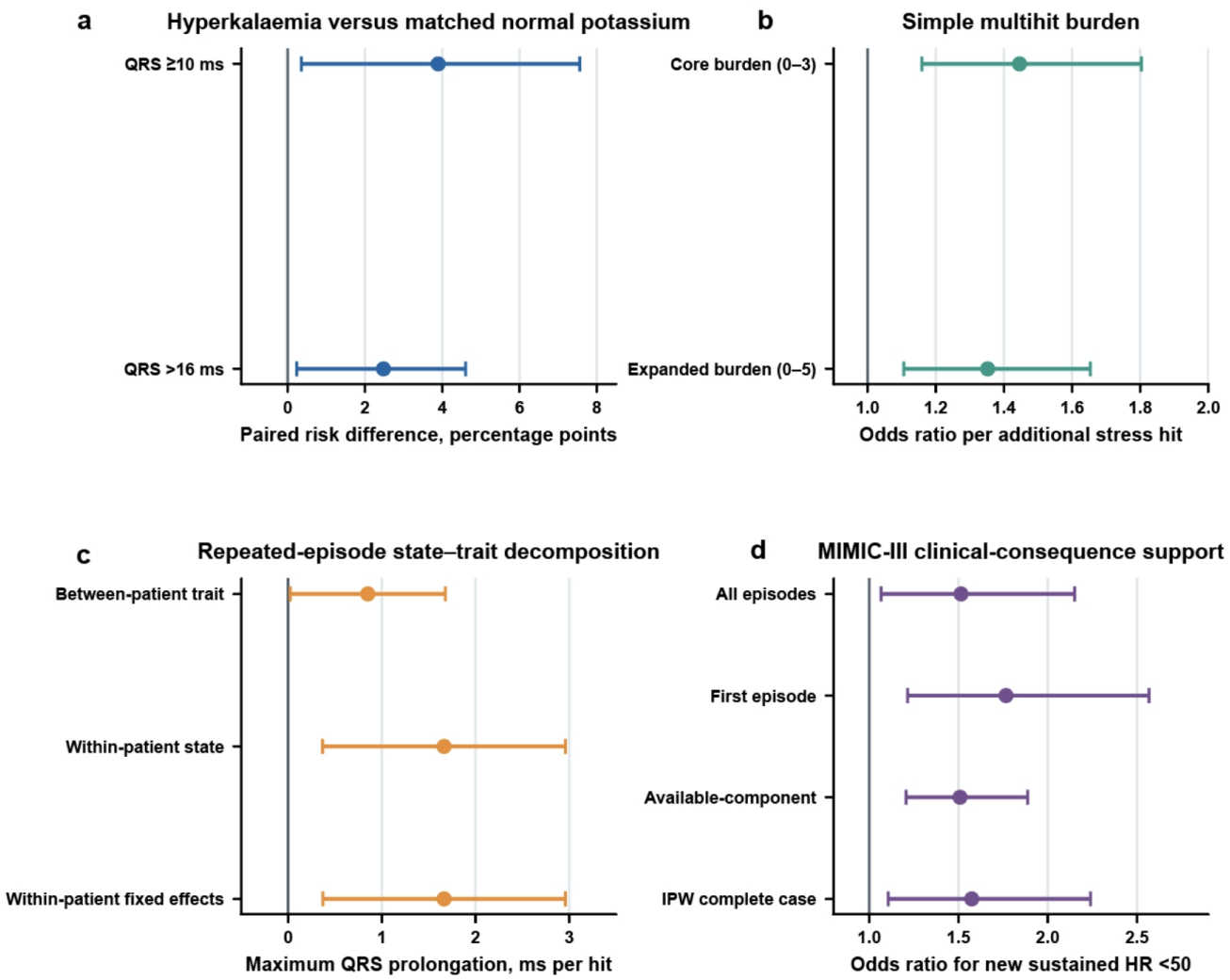


Figure 3

Triangulated support across matched normal-potassium trajectories, interpretable multihit burden, repeated-episode state–trait models, and MIMIC-III clinical consequences.

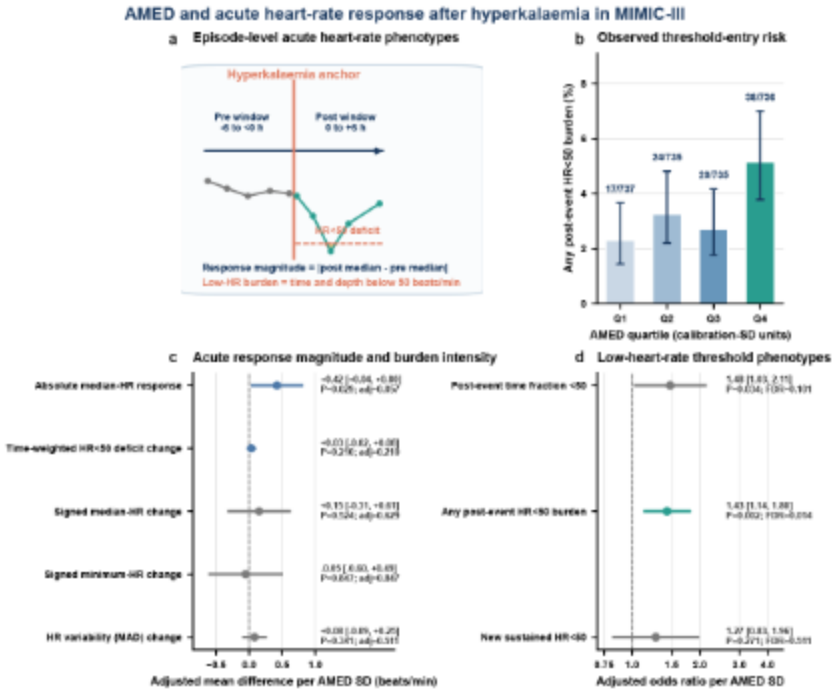


Figure 4

AMED, acute heart-rate response, and low-heart-rate burden in MIMIC-III. The multiplicity-robust signal concerned any post-event HR<50 exposure rather than sustained or cumulative burden.